J. Plasma Physics (2013), *vol.* 79, *part* 5, *pp.* 867–871. © Cambridge University Press 2013
doi:10.1017/S0022377813000615

The effect of helium impurity addition on current sheath speed in argon-operated plasma focus using a tridimensional magnetic probe

N. PANAHI[1], M. A. MOHAMMADI[2,3], S. HEDYEH[2] and R. S. RAWAT[4]

[1]Department of Physics, Islamic Azad University, Bandar Abbas Branch, P.O. Box 79159-1311, Bandar Abbas, Iran
[2]Department of Atomic and Molecular Physics, Faculty of Physics, University of Tabriz, Tabriz, Iran
(mohammadidorbash@yahoo.com)
[3]Research Center of Astrophysics and Applied Physics, University of Tabriz, Tabriz, Iran
[4]Natural Sciences and Science Education, National Institute of Education, Nanyang Technological University, Singapore

(Received 1 March 2013; revised 24 April 2013; accepted 2 May 2013; first published online 14 June 2013)

Abstract. Using the tridimensional magnetic probe, the current sheath velocity at 0.25 Torr is studied in Sahand, a Filippov-type plasma focus facility. The current sheath velocity in argon-filled plasma focus with different percentages of helium impurity at different operating voltages was studied. The highest average current sheath velocity of 12.26 ± 1.51 cm μs^{-1} at the top of the anode in the axial phase was achieved at 17 kV. Minimum average current sheath velocity is 5.24 ± 1.18 cm μs^{-1} at 12 kV with 80% argon + 20% helium as a working gas. The full width at half-maximum of peaks of the magnetic probe was found to be inversely related to the current sheath velocity, i.e. smaller at higher voltages for different impurity and decreased with increasing of impurity.

1. Introduction

The plasma focus is a simple device that makes use of a self-generated magnetic field for compressing the plasma to very high densities ($\approx 10^{25}-10^{26}$ m^{-3}) and high temperature (1–2 keV; Filippov et al. 1962; Mather 1964), and has been recognized as one of the most intense sources of fusion neutrons. The literature has often cited plasma focus as an alternative magnetic fusion device due to the intense bursts of neutrons it produces when operated in deuterium (Cloth and Conrads 1977; Brunelli and Leotta 1982). However, the plasma focus device is not only a source of fusion neutrons (Mather 1965; Soto et al. 2008; Verma et al. 2009) but it also produces highly energetic ions (Sadowski et al. 1988; Ghareshabani and Mohammadi 2012), relativistic electrons (Patran et al. 2006), and abundant amount of soft and hard X-rays (Zakaullah et al. 2002a, b; Shafiq et al. 2003; Bhuyan et al. 2004; Mohammadi et al. 2007). One of the applications of plasma focus is a pump source for lasers (Kozlov et al. 1974). Highly energetic ions from the plasma focus device have also been used extensively for material processing in the form of inducing change of phase in thin film and ion implantation as well as for deposition of thin films (Srivastava et al. 1997; Rawat et al. 2000, 2004; Soh et al. 2004; Valipour et al. 2012). Highly energetic electrons from a high repetition rate, high-performance compact plasma focus device have also been used for soft X-ray lithography (Lee et al. 2003). An important part of experimental studies on X-ray and particle emission from dense plasma focus (DPF) is oriented to interesting applications such as contact microscopy, X-ray and electron beam lithography, X-ray radiography, and micromachining (Kato and Be 1986; Beg et al. 2000; Gribkov et al. 2002; Wong et al. 2004). It has been widely reported that the production of neutrons, X-rays, and charge particle beams from the DPF is solely related to the dynamics of the collapsing current sheath at the top of the electrode assembly of the device (Decker et al. 1983; Kwek et al. 1990). The discharge current magnitude and its behavior in time are the main macroscopic parameters characterizing the plasma current sheath dynamics and the process of plasma focus formation. Typically, magnetic probes have been employed for the investigation of current sheath dynamics and its properties (Mohammadi et al. 2009; Krauz et al. 2010, 2012). The magnetic probe is a simple device to study the current sheath dynamics and its evolution in the plasma focus device.

The influence of impurities is of great interest for plasma focus community as it has been reported that their presence affects the X-ray (Verma et al. 2008) and neutron yield (Verma et al. 2009; Mohammadi et al. 2011) from the plasma focus devices and also leads to the formation of the micropinch (Koshelev et al. 1988), stabilized pinch column (Kies et al. 2000), and promotion of slipping of the current sheath due to the Hall effect near the anode (Vikherev and Braginski 1986). According to

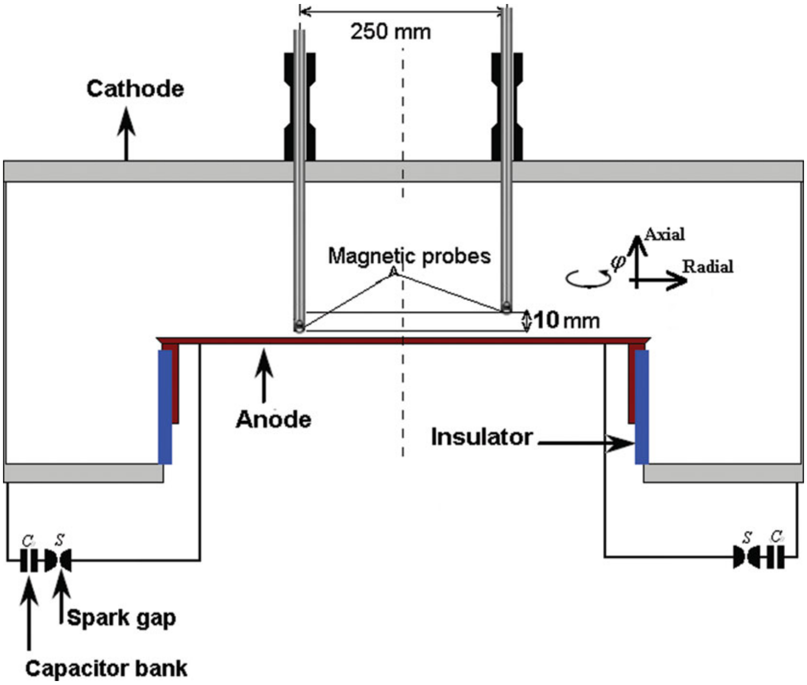

Figure 1. (Colour online) The schematic view of Sahand plasma focus.

Verma et al. (2008, 2009), the addition of high-Z krypton impurity to deuterium-enhanced X-rays and neutron yields many folds as it broadened the optimum pressure regime and stabilized the pinch for longer duration due to the slowing down of current sheath with a high-Z admixture operation, which was also observed in the POSEIDON plasma focus facility for a D_2–Ar admixture operation (Schmidt et al. 1994). The slowing down of current sheath speed in the radial phase was qualitatively deduced through an increase in the full width at half-maximum of the dip in the current derivative signal. A more precise measurement and characterization of the current sheath dynamics in the axial and radial collapse phases thus is an important diagnostics to understand the effect of impurity on the current sheath dynamics and other associated phenomenon. The tridimensional magnetic probe method, used in the investigation, offers a simple and effective alternative to a more complex and resource-intensive optical diagnostics. It may be noted that in the present investigation, the experiments were not conducted on deuterium mixed with impurity gas but on argon mixed with helium as impurity gas as the main aim was to investigate the effect of impurity on current sheath velocity using the tridimensional magnetic probe and not on the radiation emission yields.

In this paper, we study the current sheath velocity in the plasma focus device. The effect of helium gas impurity on the current sheath dynamics of an argon-operated plasma focus at different operating voltages is investigated. The purpose was to study current sheath velocities simultaneously in two dimensions, i.e. the axial and radial components, with the tridimensional magnetic probe.

2. Experimental setup

The present investigation was performed at the Sahand plasma focus facility, which is located at the University of Tabriz (Krauz et al. 2010). The schematic of the Sahand plasma focus facility is shown in Fig. 1. It is a Filippov-type plasma focus device with a maximum energy of 90 kJ at a maximum charging voltage of 25 kV. The capacitor bank consists of 24 capacitors, each with 12 μ F and a charging voltage rating of 25 kV. Capacitors are connected in parallel with a total capacitance of 288 μF. In our investigation, the device was operated at a charging voltage ranging between 12 and 17 kV. The typical maximum current in this experiment is about 1 MA. The electrode system consists of a copper disk anode of 50-cm diameter and a stainless steel cathode of 76-cm diameter serves as an outer electrode. The insulator is a cylindrical ceramic of 48 cm diameter and 11 cm length. The device was evacuated to a vacuum (10^{-3} Torr) by a rotary pump and was filled with argon and mixed with helium gas to a particular pressure (0.25 Torr) before the operation.

Magnetic probes are useful tools for sensing magnetic field structures in plasmas, especially those generated by means of fast electrical discharges. They are inexpensive and relatively simple to construct, and have been widely used in many laboratories. The magnetic probe is an inductive coil made by winding a thin gauge of wire. The voltage, $V(t)$, induced on the probe is proportional to the time derivative of the magnetic flux through the sensing coil, that is

$$V(t) = -nA\frac{dB}{dt}, \qquad (1)$$

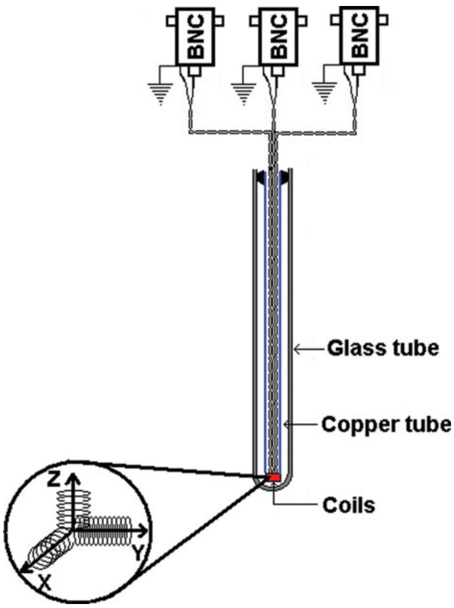

Figure 2. (Colour online) The schematic view of the magnetic probe.

where A is the area of the coil, B is the magnetic field, and n is the number of turns of coils. The tridimensional magnetic probe contains three mutually perpendicular coils in three dimensions, with each being a 10-turn coil made by winding 'SWG46' enameled copper wire onto a small plastic sleeve of about 0.65 mm diameter. The small size of the probe ensured very small disturbance to the current sheet. Two sets of tridimensional probes were used and placed at a fixed distance from each other at the top of the anode for studying plasma current sheath velocities at different voltages in the discharge volume. The schematic of the tridimensional probe is shown in Fig. 2. Using this magnetic probe, we can detect current sheath in three dimensions simultaneously. Tridimensional magnetic probes are located at the top of the anode (shown in Fig. 1), separated by 25 cm, and placed symmetrically along the radial direction for detecting the current sheath in both the radial and axial directions.

The discharge current and current derivative measurements are performed with the Rogowski coil. The coil is placed around the anode, so that the solenoid turn planes will be perpendicular to the B_φ component of the discharge current field. There is a conductor inside the polyethylene tube, which plays the role of a feedback loop for compensating the signal induced upon the large turn of the solenoid.

3. Results and discussion

In this paper, for studying the current sheath dynamics under different conditions, we operated the Sahand plasma focus device at different voltages for different mixture of gases at a fixed operating pressure of 0.25 Torr. For studying the current sheath velocity, magnetic probes were placed at different distances from the top of the anode. In Fig. 3, typical signals of current, current derivative, and magnetic probes (in one of the directions) are shown. A dip in the current derivative signal is associated with focusing of the plasma column. This is due to the rapid increase in inductance at pinching. The peak in the magnetic probe signals is associated with the passing by of the current sheath through the magnetic probe location. As the magnetic probes are located at a different axial distance from the top of the anode, magnetic probe signals gets separated in time. As the time difference was estimated from the oscilloscope signals and using the axial distance of the separation between the magnetic probes, the average current sheath speeds were calculated. The variation of the current sheath velocity at the top of the anode surface in the radial phase is shown in Fig. 4. The maximum average speed is 12.26 ± 1.51 cm μs^{-1} for argon at 17 kV. At 12 kV with 80% argon + 20% helium as a working gas, the minimum average speed is 5.24 ± 1.18 cm μs^{-1}. This figure shows that at higher voltage the speed is increased. At higher voltages, the discharge current is higher, resulting in a greater magnetic force on the current sheath and hence it will move faster. Another notable result is the effect of impurity on the average current

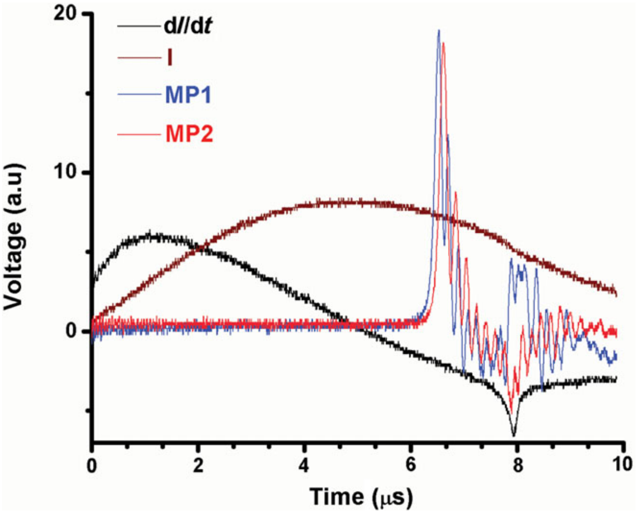

Figure 3. (Colour online) Typical signal of the magnetic probes, current, and current derivative.

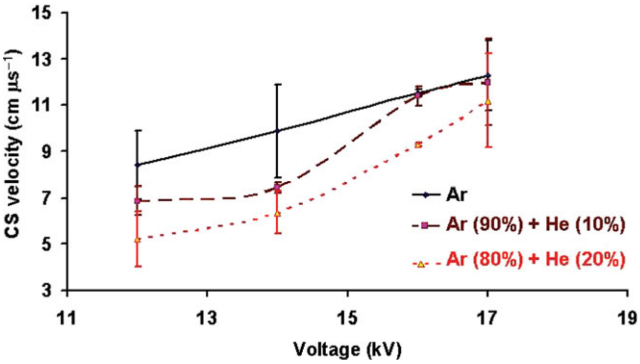

Figure 4. (Colour online) Variation of the current sheath velocity at the top of the anode surface in the radial phase.

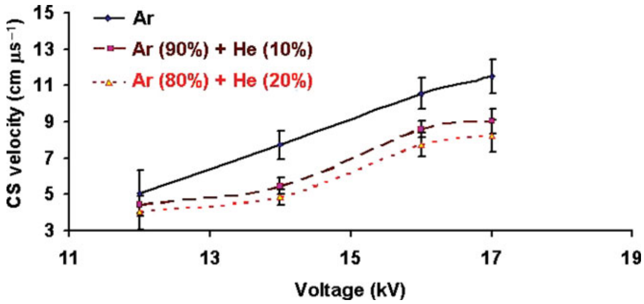

Figure 5. (Colour online) Variation of the current sheath velocity at the top of the anode surface in the axial phase.

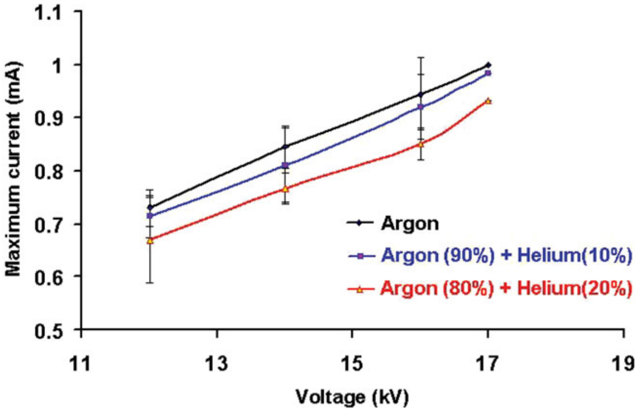

Figure 6. (Colour online) Variation of maximum current with charging voltage.

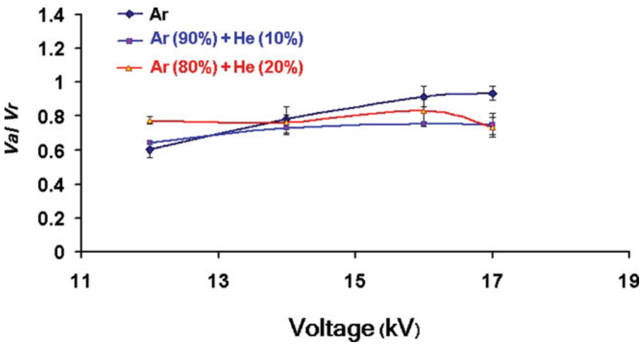

Figure 7. (Colour online) The ratio of axial to radial CS velocity, (v_a/v_r), as a function of charging voltage.

sheath speed. With increasing impurity, the average current sheath speed decreases.

In Fig. 5, the variation of the average current sheath speed with working voltages in the axial phase at the top of the anode surface is shown. In the axial phase, the maximum average speed is 11.48 $\pm$ 0.92 cm μs^{-1} in 17 kV as a working voltage with argon. The minimum average current sheath (CS) speed during the axial phase is found to be 5.08 $\pm$ 1.28 cm μs^{-1} for 80% argon + 20% helium as the working gas at 12 kV. Like the radial phase, the average axial CS speed at all voltages with argon is more than at gas mixtures.

It is interesting to note that for the axial and the radial phases, the current sheath speeds decrease with the increasing impurity helium gas admixture ratio. This is in contradiction to our expectation, as the addition of low-mass-number helium impurity in high-mass-number argon background gas is expected to result in higher current sheath speed as the net mass to be swept by the current sheath is lower. Further investigation was performed to provide the plausible explanation for this observation.

Figure 6 shows the variation of maximum current (i.e. the peak discharge current flowing through the plasma focus device) as a function of charging voltage for three different gas combinations. The figure shows that with increasing charging voltage, the maximum current discharge through the plasma increases. Figure 6 also shows that at each of the charging voltages the maximum current (i.e. the peak discharge current flowing through the plasma focus device) decreases with increasing helium impurity content. The decrease in maximum current would lead to the decrease in the fraction, fc, of the current flowing through the current sheath, and hence the corresponding magnetic field and the Lorentz force will be lower, resulting in lower current sheath speed. It may be difficult to provide the exact reason for the decrease in maximum current (or corresponding fc) with increasing helium impurity concentration in argon, but it may be hypothesized that the higher ionization energy of helium compared with that argon (e.g. first ionization of helium is 24.58 eV while that of argon is 15.75 eV) may result in lower ionization efficiency (in particular, during the axial rundown phase) and hence the lower current coupling efficiency in helium–argon admixture operation.

The ratio of the average CS speed of the radial phase to the axial phase (v_a/v_r) is shown in Fig. 7. This figure shows that at all voltages$v_a < v_r$, which is in agreement with that commonly reported in the literature. This means that a greater fraction of current passes through the current sheath during the radial/pinch phase, resulting in greater acceleration and hence a greater average CS speed. The plasma temperature during the radial phase is known to increase to hundreds of eV, leading to a very high degree of ionization of the filling gas. Hence, the current coupling fraction, fc, during the radial collapse phase can be significantly higher than the axial phase, leading to an increase in current sheath speed in the radial phase.

4. Conclusion

Using the tridimensional magnetic probe, the average current sheath speed in two dimensions in a Filippov-type Sahand plasma focus is studied simultaneously. The effect of impurity on the current sheath velocity shows that, by adding helium as an impurity into the argon, the current sheath velocity decreases. The maximum average speed of 12.26 $\pm$ 1.51 cm μs^{-1} was achieved at 17 kV with argon as a working gas during the radial phase. The minimum average current sheath speed during the radial phase is 5.24 $\pm$ 1.18 cm μs^{-1} with

80% argon + 20% helium at 12 kV. In the axial phase, the maximum current sheath speed is 11.48 ± 0.92 cm μs^{-1}at 17 kV as a working voltage with argon. The minimum average speed achieved in the axial phase was 5.08 ± 1.28 cm μs^{-1} for 80% argon + 20% helium as a working gas at 12 kV. The average current sheath speed at all voltages in the radial phase is greater than that in the axial phase at the top of the anode. It is also concluded that the maximum current flowing into the current sheath is strongly related on the purity of gas. We find that with the increasing concentration of helium as an impurity into the argon as a working gas, the maximum current and the current sheath speed are decreased.

References

Beg, F. N., Ross, I., Lorena, A., Worley, J. F., Danger, A. E. and Hanies, M. G. 2000 *J. Appl. Phys.* **88**, 3225.

Bhuyan, H., Mohanty, S. R., Neagy, N. K., Bujarbarua, S. and Rout, R. K. 2004 *J. Appl. Phys.* **95**, 2975.

Brunelli, B. and Leotta, G. 1982 *Unconventional Approach to Fusion*. New York: Plenum, 157 pp.

Cloth, P. and Conrads, H. 1977 *Nucl. Sci. Engg.* **62**, 591.

Decker, G., Kies, W. and Pross, G. 1983 *Phys. Fluids* **26**, 571.

Filippov, N. V., Filippova, T. I. and Vinogradov, V. P. 1962 *Nucl. Fusion Suppl.* **2**, 77.

Ghareshabani, E. and Mohammadi, M. A. 2012 *J. Fusion Energy* **31**, 595.

Gribkov, V. A., Srivastava, A., Keat, P. L. C., Kudryashov, V. and Lee, S. 2002 *IEEE Trans. Plasma Sci.* **30**, 1331.

Kato, Y. and Be, S. H. 1986 *Appl. Phys. Lett.* **48**, 686.

Kies, W., Decker, G., Berntien, U., Sidelnikov, Y. V., Glushkov, D. A., Koshelev, K. N., Simanovskii, D. M. and Babashev, S. V. 2000 *Plasma Sources Sci. Technol.* **9**, 27.

Koshelev, K. N., Krauz, V. I., Reshetniak, N. G., Salukvadze, R. G., Sidelnikov, Yu. V. and Khautiev, E. Yu. 1988 *J. Phys. D: Appl. Phys.* **21**(12), 1827.

Kozlov, N. P., Aleksev, V. A., Protsov, Y. S. and Rubinov, A. B. 1974 *JEPT Lett.* **20**, 331.

Krauz, V., Mitrofanov, K., Myalton, V. V., Grabovski, E. V., Koidan, V. S., Vinogradov, V. P., Vinogradova, Y. V. and Zukakishvili, G. G. 2010 *IEEE Trans. Plasma Sci.* **38**, 92.

Krauz, V., Mitrofanov, K., Scholz, M., Paduch, M., Karpinski, L., Zielinska, E. and Kubes, P. 2012 *Plasma Phys. Control. Fusion* **54**, 025010.

Kwek, K. H., Tou, T. Y. and Lee, S. 1990 *IEEE Trans. Plasma Sci.* **18**, 826.

Lee, S., Lee, P., Zhang, G., Serban, A., Liu, M., Liu, X., Feng, X., Springham, S. V., Selvam, C. S., Kudryashov, V. and Wong, T. K. S. 2003 *Sing. J. Phys.* **173**, 276.

Mather, J. W. 1964 *Phys. Fluids* **7**, 5.

Mather, J. W. 1965 *Phys. Fluids* **8**, 366.

Mohammadi, M. A., Sobhanian, S., Ghomeshi, M., Ghareshabani, E., Moslehi-fard, M., Lee, S. and Rawat, R. S. 2009 *J. Fusion Energy* **28**, 371.

Mohammadi, M. A., Sobhanian, S. and Rawat, R. S. 2011 *Phys. Lett.* A **375**, 3002.

Mohammadi, M. A., Verma, R., Sobhanian, S., Wong, C. S., Lee, S., Springham, S. V., Tan, T. L., Lee, P. and Rawat, R. S. 2007 *Plasma Sour. Sci. Tech.* **16**, 785.

Patran, A., Stoenescu, D., Rawat, R. S., Springham, S. V., Tan, T. L., Tan, T. L., Rafique, M. S., Lee, P. and Lee, S. 2006 *J. Fusion Energy* **25**, 57.

Rawat, R. S., Arun, P., Vedeshwer, A. G., Lam, Y. L., Liu, M. H., Lee, P. and Lee, S. 2000 *Mater. Res. Bull.* **35**, 477.

Rawat, R. S., Arun, P., Vedeshwer, A. G., Lee, P. and Lee, S. 2004 *J. Appl. Phys.* **95**, 7725.

Sadowski, M., Zebrowski, J., Rydygier, E. and Kucinski, J. 1988 *Plasma Phys. Contr. Fusion* **30**, 763.

Schmidt, H., Sadowski, M., Jakubowski, L., Sadowska, E. S. and Stanislawski, J. 1994 *Plasma Phys. Control. Fusion* **36**, 13.

Shafiq, M., Hussain, S., Waheed, A. and Zakaullah, M. 2003 *Plasma Sour. Sci. Tech.* **12**, 199.

Soh, L. Y., Lee, P., Shuyan, X., Lee, S. and Rawat, R. S. 2004 *IEEE Trans. Plasma Sci.* **32**, 448.

Soto, L., Silva, P., Moreno, J., Zambra, M., Kies, W., Mayer, R. E., Clausse, A., Altamirano, L., Pavez, C. and Huerta, L. 2008 *J. Phys. D: Appl. Phys.* **41**, 205215.

Srivastava, M. P., Mohanty, S. R., Annapoorni, S. and Rawat, R. S. 1997 *Phys. Lett.* A **231**, 434.

Valipour, M., Mohammadi, M. A., Sobhanian, S. and Rawat, R. S. 2012 *J. Fusion Energy* **31**, 65.

Verma, R., Lee, P., Lee, S., Springham, S. V., Tan, T. L., Krishnan, M. and Rawat, R. S. 2009 *Appl. Phys. Lett.* **93**, 101501.

Verma, R., Lee, P., Lee, S., Springham, S. V., Tan, T. L., Rawat, R. S. and Krishnan, M. 2008 *Appl. Phys. Lett.* **93**, 101501.

Vikherev, V. V. and Braginski, S. I. 1986 *Rev. Plasma Phys.* **10**, 425.

Wong, D., Patran, A., Tan, T. L., Rawat, R. S. and Lee, P. 2004 *IEEE Trans. Plasma Sci.* **32**, 2227.

Zakaullah, M., Alamgir, K., Shafiq, M., Hassan, S. M., Sharif, M., Hussain, S. and Waheed, A. 2002a *Plasma Sour. Sci. Tech.* **11**, 377.

Zakaullah, M., Alamgir, A., Shafiq, M., Sharif, M. and Waheed, A. 2002b *IEEE Trans. Plasma Sci.* **30**, 2089.